Optics Communications 435 (2019) 68–74

Contents lists available at ScienceDirect

Optics Communications

journal homepage: www.elsevier.com/locate/optcom

Investigating the displacement resolution of laser heterodyne detection system

Yan Chun-Hui [a,b], Wang Ting-Feng [a,*], Li Yuan-Yang [a], Lv Tao [a,b], Wu Shi-Song [a,b]

[a] State Key Laboratory of Laser Interaction with Matter, Changchun Institute of Optics, Fine Mechanics and Physics, Chinese Academy of Sciences, Changchun 130033, China

[b] University of Chinese Academy of Sciences, Beijing 100049, China

ARTICLE INFO

Keywords:
Heterodyne detection
Laser applications
Phase noise

ABSTRACT

In this paper, we provide a fairly standard derivation of the power spectrum of photocurrent and limited displacement resolution of laser heterodyne detection system. And the phase noise with different oscillation lineshapes of the heterodyne detection system is discussed. Based on the one-dimensional probability distribution model of phase noise, the minimum resolvable displacement and noise-equivalent mean square displacement are established, which represent the minimum detectable amplitude and noise limited resolution respectively. According to the numerical results, we obtain the variation of displacement resolution against the key parameters including the laser wavelength, the detection distance, the laser linewidth and the signal power. It reveals that the phase fluctuation has a significant effect on the power spectrum of photocurrent. Besides, both the probability density distribution of phase noise and displacement resolution have heavy dependence on laser oscillation lineshapes. And the noise-equivalent mean square displacement is inversely proportional to the root-mean-square of a measurable light power. The noise-equivalent mean square displacement can reach $3.5\times10^{-15}\mathrm{m}/\sqrt{\mathrm{Hz}}$ under the given parameters. Our findings provide a quantitative reference for the displacement resolution and engineering application of the heterodyne detection.

1. Introduction

The heterodyne detection is a widely used technique in the microwave region developed by researchers for many years, which has advantages in high-precision, non-contact and anti-interference vibration measurements with nanometric scale. The heterodyne detection technique has good prospects of applications in micro-vibration and velocity measurement, rotation target spectrum identification and laser ultrasonic propagation imager. Several excellent reviews [1–3] in the 1960s describing the detection of micro-vibration with homodyne techniques were limited to small-amplitude vibrations (<25 nm) or could only be able to detect a standard sinusoidal vibration. Then the measurement of vibrating surfaces by laser Doppler technique proved to be available with crucial developments of heterodyne techniques [4,5] during the 1980s. Typical systems of the heterodyne detection technique include Firepond radar [6] and HI-CLASS system [7] researched by MIT Lincoln lab and Air Force Research Laboratory, respectively.

As optical frequencies in the range of 10^{15} Hz cannot be detected directly by a photodetector, the frequency ω_1 of a measurement beam has to be mixed down by a reference beam obtained from a coherent light source with the frequency ω_2. Usually, the reference beam is shifted in the frequency domain through an acousto-optic modulator whose drive signal is offered by a signal generator [8,9]. The output current of the detector contains a component which corresponds to the heterodyne intermediate frequency. It is evident to demodulate the phase of heterodyne intermediate frequency to acquire the instantaneous vibration information.

The displacement resolution of laser heterodyne detection system not only depends on the performance of photodetector and laser source but also the rest of the system, such as the acousto-optic modulator, the fiber circulator, the target surface roughness and the matching progress of signal light and local oscillator light. However, the former are dominant and the latter can be converted into the signal–noise ratio. Consequently, taking the formers into account is enough to illustrate the issue of the displacement resolution of heterodyne detection system. For a long-range heterodyne detection over several hundred meters or more, additional considerations including the influence of atmospheric turbulence should be given [10–12]. Although the optical heterodyne detection has been pursued for many years, there is no report of the limited displacement resolution of the heterodyne detection system.

In Section 2.1, we will derive the power spectral density by introducing the phase noise for a general heterodyne system. Since the amplitude noise of heterodyne detection is usually negligible, laser linewidths are

* Corresponding author.
E-mail address: tingfeng_w@sina.com (W. Ting-Feng).

https://doi.org/10.1016/j.optcom.2018.11.017
Received 13 March 2018; Received in revised form 25 October 2018; Accepted 6 November 2018
Available online 13 November 2018

due to the phase noise of photocurrent. It means that we can directly associate the coherent time with the laser linewidth. Subsequently we will discuss the power spectrum of phase noise.

Furthermore, we will derive the minimum resolvable displacement and noise-equivalent mean square displacement in Section 2.2.The one-dimensional probability distribution model of phase noise of heterodyne detection system is proposed. And we built up the quantitative mathematical formulas of both the minimum resolvable displacement and noise-equivalent mean square displacement for different oscillation lineshapes [13,14]. Some numerical results are presented to show the displacement resolution of heterodyne system with the key parameters including the laser wavelength λ, the laser linewidth $\Delta\omega$ (FWHM, full width at half maximum), the propagation delay time τ_d and the signal power. Finally we briefly discuss the implications of our work for the displacement resolution and engineering application of the heterodyne detection, which is the motivation of our works.

2. Theory

2.1. The power spectral density

Consider a general equation for a heterodyne detection system [15,16]

$$A_{out} = A_1 e^{i\omega_0(t-\tau_d)+i\phi(t-\tau_d)} + A_2 e^{i(\omega_0+\omega_s)t+i\phi(t)+i\phi'(t)} \tag{1}$$

A_1 and A_2 are the amplitude of the heterodyne detection signal, ω_0 is the average optical frequency and $\phi(t)$ is a stochastic process symbolizing the phase fluctuations. τ_d is the propagation delay time between the signal light and local oscillator light. ω_s is the frequency difference of the reference and measurement beams – that is the intermediate frequency signal of the heterodyne detection. ω_s is less than the cut-off response frequency f_s of photodetector, which leads to an output current from the photodetector. This equation has also included the possibility that one path could introduce its phase noise $\phi'(t)$.

The light intensity of a heterodyne detection signal will be

$$\begin{aligned} I &\propto |A_{out}|^2 \\ &\propto |A_1|^2 + |A_2|^2 + 2A_1A_2\cos\left[\omega_s t + \phi(t) - \phi\left(t-\tau_d\right) + \phi'(t) + \omega_0\tau_d\right] \end{aligned} \tag{2}$$

The photocurrent (in the complex notation) of the heterodyne detection system is written as

$$i(t) = i_1 + i_2 + 2\sqrt{i_1 i_2}e^{i[\omega_s t+\phi(t)-\phi(t-\tau_d)+\phi'(t)+\omega_0\tau_d]} \tag{3}$$

i_1 and i_2 are current components of reference beams and measurement beams respectively. In the laser heterodyne detection system over tens meters, ignoring the influence of atmospheric turbulence and target modulation, the beam from the laser is divided into reference and measurement beams with a beam splitter.

We will use the Wiener–Khinchin theorem to calculate the power spectral density of photocurrent with the phase noise. The Wiener–Khinchin theorem indicates that the power spectral density of photocurrent is the Fourier transform of its autocorrelation function. This can be summarized as

$$P(\omega) = F[R(\tau)] \tag{4}$$

$R(\tau)$ is the autocorrelation function of photocurrent.

To work out the spectrum of this photocurrent, we calculate the autocorrelation firstly

$$R(\tau) = E\left[i(t+\tau)\,i(t)^*\right] \tag{5}$$

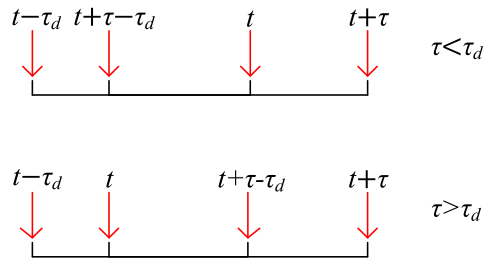

Fig. 1. Representation of the possible statistically independent (non-overlapping) intervals in the stochastic phase noise time line. Only positive values of τ are considered here but negative values should be considered also.

Continuing the calculation we get

$$\begin{aligned} R(\tau) &= \left(i_1+i_2\right)^2 \\ &+ E\left\{2\left(i_1+i_2\right)\sqrt{i_1 i_2}\left[e^{i(\omega_s(t+\tau)+\phi(t+\tau)-\phi(t+\tau-\tau_d)+\phi'(t+\tau)+\omega_0\tau_d)}\right.\right. \\ &+ \left.e^{-i(\omega_s t+\phi(t)-\phi(t-\tau_d)+\phi'(t)+\omega_0\tau_d)}\right] \\ &+ \left.4i_1 i_2 e^{i(\omega_s\tau+\phi(t+\tau)-\phi(t+\tau-\tau_d)-\phi(t)+\phi(t-\tau_d)+\phi'(t+\tau)-\phi'(t))}\right\} \end{aligned} \tag{6}$$

When working with expectations, we can use

$$E[X+Y] = E[X] + E[Y] \tag{7}$$

Even if X and Y are not statistically independent, we should consider each term separately. The second and third terms look like that they will average to zero due to the term $e^{i\omega_s t}$. The terms will be independent of τ and so can only contribute to the DC term of the spectral density (in the second term a substitution of $\varphi = t+\tau$ shows its independence from t). So, we will consider the fourth term and the phase error terms in its exponent

$$\phi(t+\tau) - \phi\left(t+\tau-\tau_d\right) - \phi(t) + \phi\left(t-\tau_d\right) \tag{8}$$

We know that the phase noise is a Wiener process and so we assume that

$$\phi(t+\tau) - \phi(t) = \Delta\phi(t,\tau) \tag{9}$$

This is a random variable in the form of Gaussian white noise. The one-dimensional probability density function of phase noise $\Delta\phi(t,\tau)$ obeys a Gaussian distribution with $\mu = 0$. The variance σ^2 is proportional to $|\tau|$ and we will define $\sigma^2 = b|\tau|$.

It can be simplified to two Gaussian white noise variables and there are two ways of doing this. Either

$$\Delta\varphi\left(t,-\tau_d\right)\big|_{t=t} - \Delta\varphi\left(t,-\tau_d\right)\big|_{t=t+\tau} \tag{10}$$

Or

$$\Delta\varphi(t,\tau)\big|_{t=t} - \Delta\varphi(t,\tau)\big|_{t=t-\tau_d} \tag{11}$$

The absolute time of the variables is shown explicitly in order to distinguish two random variables. If we want to further combine them, we need to know whether they are correlated or statistically independent. From the properties of Wiener processes, we know that the intervals will be independent as long as they do not overlap. In Fig. 1 we see that if $\tau \geq \tau_d$ the first expression ensures that the two terms are statistically independent but if $\tau \leq \tau_d$ the second expression should be used to get independent statistics. Subsequently we can get

$$\begin{aligned} \Delta\varphi\left(t,-\tau_d\right)\big|_{t=t} - \Delta\varphi\left(t,-\tau_d\right)\big|_{t=t+\tau} &= \sqrt{2}\Delta\phi\left(t,-\tau_d\right) \\ &= N\left(0,2b|\tau_d|\right) \quad |\tau| \geq \tau_d \end{aligned} \tag{12}$$

$$\Delta\varphi(t,\tau)\big|_{t=t} - \Delta\varphi(t,\tau)\Big|_{t=t-\tau_d} = \sqrt{2}\Delta\phi(t,\tau) = N(0,2b|\tau|) \quad |\tau| \leq \tau_d \tag{13}$$

We see that combining noisy variables use a different kind of mathematical rules (see Appendix A). It is not completely clear here but the same final results are found when τ is negative, hence we have included modulus signs around τ in the above expressions.

Now we note that X and Y are statistically independent

$$E[XY] = E[X]E[Y] \tag{14}$$

This means that the fourth term in Eq. (6) can become

$$4i_1i_2e^{i\omega_s\tau}E\left[e^{i\Delta\phi(t,\tau)'}\right]\begin{cases}E\left[\exp\left(i\sqrt{2}\Delta\phi(t,\tau)\right)\right] & \tau \le \tau_d\\ E\left[\exp\left(i\sqrt{2}\Delta\phi(t,-\tau_d)\right)\right] & \tau \ge \tau_d\end{cases} \tag{15}$$

$\Delta\phi(t,\tau)' = \phi'(t+\tau) - \phi'(t)$ is the contribution of the extra phase noise and there is a b' accordingly which is also the Brown noise.

We have worked out these expectations and we can get directly

$$R(\tau) = R_0 + 4i_1i_2e^{i\omega_s\tau}e^{-b'|\tau|/2}\begin{cases}e^{-b|\tau|} & \tau \le \tau_d\\ e^{-b|\tau_d|} & \tau \ge \tau_d\end{cases} \tag{16}$$

R_0 is equal to $(i_1+i_2)^2$or something else for dc due to the neglected second and third terms. This can be written as

$$R(\tau) = R_0 + 4i_1i_2e^{i\omega_s\tau}e^{-b'|\tau|/2}\left(e^{-b|\tau_d|} + rect\left(\frac{\tau}{2\tau_d}\right)\left(e^{-b|\tau|} - e^{-b|\tau_d|}\right)\right) \tag{17}$$

$rect(x)$ is the rectangular function which is equal to 1 for $-0.5 < x < 0.5$ and zero elsewhere. We now get the power spectral density by the Fourier transform of its autocorrelation function.

$$\begin{aligned}&F[R(\tau)] = R_0 2\pi\delta(\omega) + 4i_1i_2 2\pi L(\omega-\omega_s,b')e^{-b|\tau_d|}\\ &+4i_1i_2L(\omega-\omega_s,b') * \left\{\int_{-\tau_d}^{\tau_d}\left(e^{-b|\tau|} - e^{-b|\tau_d|}\right)e^{-i\omega\tau}d\tau\right\}\end{aligned} \tag{18}$$

$L(\omega,\Delta\omega)$ is a Lorentzian function centered at 0 and with a linewidth (FWHM) of $\Delta\omega$.

$$L(\omega,\Delta\omega) = \frac{1}{\pi}\frac{\Delta\omega/2}{(\Delta\omega)^2/4+\omega^2} \tag{19}$$

Now consider this notation

$$\int_{-\tau_d}^{\tau_d}\left(e^{-b|\tau|} - e^{-b|\tau_d|}\right)e^{-i\omega\tau}d\tau \tag{20}$$

To simplify it we treat τ_d as positive

$$\begin{aligned}&2F\left[\int_0^{\tau_d}e^{-b\tau}e^{-i\omega\tau}d\tau\right] - e^{-b\tau_d}\int_{-\tau_d}^{\tau_d}e^{-i\omega\tau}d\tau\\ &= 2F\left[\frac{e^{-b\tau_d}e^{-i\omega\tau_d}-1}{-b-i\omega}\right] - e^{-b\tau_d}\left\{\frac{e^{-i\omega\tau_d}-e^{i\omega\tau_d}}{-i\omega}\right\}\\ &= 2F\left[\frac{b\left(1-e^{-b\tau_d}e^{-i\omega\tau_d}\right)+i\omega\left(e^{-b\tau_d}e^{-i\omega\tau_d}-1\right)}{b^2+\omega^2}\right] - 2e^{-b\tau_d}\frac{\sin(\omega\tau_d)}{\omega}\\ &= 2\frac{b\left(1-e^{-b\tau_d}\cos(\omega\tau_d)\right)+\omega e^{-b\tau_d}\sin(\omega\tau_d)}{b^2+\omega^2} - 2e^{-b\tau_d}\frac{\sin(\omega\tau_d)}{\omega}\end{aligned} \tag{21}$$

This Eq. (21) according to Eq. (19) can be simplified to

$$2\pi L(\omega,2b)\left\{1 - e^{-b\tau_d}\left[\cos(\omega\tau_d) + \frac{b}{\omega}\sin(\omega\tau_d)\right]\right\} \tag{22}$$

Therefore, the power spectral density is

$$\begin{aligned}&P(\omega) \propto R_0 2\pi\delta(\omega) + 4i_1i_2 2\pi L(\omega-\omega_s,b')e^{-b\tau_d} + 4i_1i_2L(\omega-\omega_s,b')\\ &* \left\{2\pi L(\omega,2b)\left[1 - e^{-b\tau_d}\left(\cos(\omega\tau_d) + \frac{b}{\omega}\sin(\omega\tau_d)\right)\right]\right\}\end{aligned} \tag{23}$$

Note also that if $b \to 0$ then $L(\omega-\Delta\omega,b') \to \delta(\omega-\Delta\omega)$

2.2. The displacement resolution

From Section 2.1 there are three components included in the light intensity of a heterodyne detection signal and so each photocurrent comprises three components. First two terms are proportional to the individual power of each interference field, while the third one is proportional to a coherent term that depends on the phase of the photocurrent. The balanced detection is an effective suppression of the local oscillator intensity noise in the heterodyne detection. However, dominant noise sources are not eliminated by means of the balanced detection and a careful matching of the carrier frequencies is necessary to avoid a severe system impairment. The photodiodes are connected together to provide the differential current [17], (See Fig. 2.)

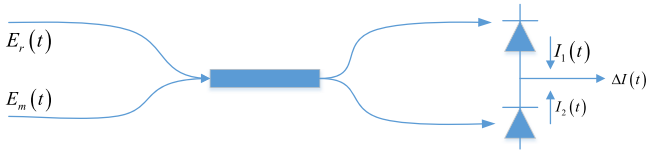

Fig. 2. Basic configuration for balanced detection.

$$\begin{aligned}I_1(t) &= K\left\{\frac{E_r^2}{2} + \frac{E_m^2}{2} + E_rE_m\cos\left[\omega_st + \varphi(t+\tau_d) - \varphi(t)\right]\right\}\\ I_2(t) &= K\left\{\frac{E_r^2}{2} + \frac{E_m^2}{2} - E_rE_m\cos\left[\omega_st + \varphi(t+\tau_d) - \varphi(t)\right]\right\}\\ \Delta I(t) &= I_1(t) - I_2(t) = 2K\sqrt{P_r(t)P_m(t)}\cdot\cos\left[\omega_st + \varphi(t+\tau_d) - \varphi(t)\right]\end{aligned} \tag{24}$$

K is the conversion parameter $K = \eta q/h\upsilon$, h is the Planck constant, υ is the optical frequency, η is the quantum efficiency and q is the charge of an electron. E_r and E_m are amplitudes of the reference and measurement beams respectively. $I_1(t)$ and $I_2(t)$ are output differential currents of the balanced detector. P_r and P_m are the optical powers of the reference and measurement beams respectively, ω_s is the angular frequency of intermediate frequency signal and $\phi(t)$ is phase fluctuations caused by the laser linewidth. And

$$\omega_st = \frac{4\pi s(t)}{\lambda} + 2\pi f_{AOM}t \tag{25}$$

$s(t)$ is the target vibration signal that we try to acquire. And frequency fluctuations of the laser can convert into the phase noise according to the signal and noise theory mentioned above. After the quadrature demodulation algorithm we can obtain two quadrature I&Q signals.

$$\begin{aligned}I(t) &= \left[\Delta I(t)\times\sin\left(2\pi f_{AOM}t\right)\right] * h_{LPF}\\ &= K\sqrt{P_r(t)P_m(t)}\cos\left(\frac{4\pi s(t)}{\lambda} + \phi(t+\tau_d) - \phi(t)\right)\\ Q(t) &= \left[\Delta I(t)\times\cos\left(2\pi f_{AOM}t\right)\right] * h_{LPF}\\ &= K\sqrt{P_r(t)P_m(t)}\sin\left(\frac{4\pi s(t)}{\lambda} + \phi(t+\tau_d) - \phi(t)\right)\end{aligned} \tag{26}$$

f_{AOM} is the frequency of AOM and h_{LPF}denotes the function of low-pass filter. Through an arctangent approach and removing the coefficient we can get the phase caused by the target vibration

$$\phi = \frac{4\pi s(t)}{\lambda} + \phi(t+\tau_d) - \phi(t) \tag{27}$$

We consider the phase noise as a Wiener process, which obeys a Gaussian distribution with zero-mean-value

$$f[\Delta\phi(t,\tau)] = \frac{1}{\sqrt{2\pi\sigma^2}}e^{-[\Delta\phi(t,\tau)]^2/2\sigma^2} \tag{28}$$

The variance of phase noise is different in the Gauss spectrum and Lorentz spectrum due to laser oscillation lineshapes [13]

$$\begin{aligned}\sigma_{\text{Gauss}}{}^2 &= \left\langle\left(\phi(t+\tau_d) - \phi(t)\right)^2\right\rangle = \left(2\pi\Delta\omega_{\text{Gauss}}\right)^2\tau_d^2\\ \sigma_{\text{Lorentz}}{}^2 &= \left\langle\left(\phi(t+\tau_d) - \phi(t)\right)^2\right\rangle = 2\pi\Delta\omega_{\text{Lorentz}}\tau_d\end{aligned} \tag{29}$$

The delay time $\tau_d = 2d/c$, d is the detection distance, c is the velocity of light, $\Delta\omega_{\text{Gauss}}$ is the lineshape of the Gauss spectrum and $\Delta\omega_{\text{Lorentz}}$ is

the lineshape of the Lorentz spectrum. Then we can get the probability distribution model of phase noise expressed by

$$\begin{aligned} f_{Gauss}\left[\Delta\phi(t,\tau)\right] &= \frac{1}{\sigma_{\text{Gauss}}\sqrt{2\pi}} e^{\left(-\frac{(\Delta\phi(t,\tau)-\mu)^2}{2\sigma_{\text{Gauss}}{}^2}\right)} \\ &= \frac{1}{2\pi\tau_d\Delta\omega_{\text{Gauss}}\sqrt{2\pi}} e^{\left(-\frac{[\Delta\phi(t,\tau)]^2}{2\times\left(2\pi\tau_d\Delta\omega_{\text{Gauss}}\right)^2}\right)} \\ f_{\text{Lorentz}}\left[\Delta\phi(t,\tau)\right] &= \frac{1}{\sqrt{2\pi}\sigma_{\text{Lorentz}}} e^{\left(-\frac{(\Delta\phi(t,\tau)-\mu)^2}{2\sigma_{\text{Gauss}}{}^2}\right)} \\ &= \frac{1}{2\pi\cdot\sqrt{\tau_d\Delta\omega_{\text{Lorentz}}}} e^{\left(-\frac{[\Delta\phi(t,\tau)]^2}{2\times2\pi\tau_d\Delta\omega_{\text{Lorentz}}}\right)} \end{aligned} \tag{30}$$

The Gaussian distribution obeys '3σ standards' which is that the probability in the range $(\mu-\sigma,\mu+\sigma)$ is 68.27%, the probability in the range $(\mu-2\sigma,\mu+2\sigma)$ is 95.45% and the probability in the range $(\mu-3\sigma,\mu+3\sigma)$ is 99.74%. We can believe that the value of $\Delta\phi$ is almost concentrated in the range of $(\mu-3\sigma,\mu+3\sigma)$. The probability beyond this range does not exceed 0.3%. We can get the worst demodulation result.

$$\begin{aligned} \phi_{\text{Gauss}} &= \phi_s \pm 3\sigma_{\text{Gauss}} = \frac{4\pi s(t)}{\lambda} \pm \frac{12\pi d}{c}\Delta\omega_{\text{Gauss}} \\ \phi_{\text{Lorentz}} &= \phi_s \pm 3\sigma_{\text{Lorentz}} = \frac{4\pi s(t)}{\lambda} \pm 3\cdot\sqrt{\frac{4\pi d}{c}\Delta\omega_{\text{Lorentz}}} \end{aligned} \tag{31}$$

We establish linkages between the vibrations of target and the phase noise of photocurrent. Basically, there are three ultimate sources of noise in the signal process of a laser heterodyne detection system: shot noise, thermal noise of the detector or preamplifier combination and quantization noise. Here taking the above observations into account, physical limits are set here by the quantum nature of light generating shot noise which is usually the dominant noise source.

The photocurrent consists of a direct-current component proportional to the total optical power $P_r + P_m$ and an alternating current component with a mean square value representing the power of the heterodyne carrier signal. The total power $P_r + P_m$ not only generates a DC component but also produces the shot noise described by the mean square noise current

$$\bar{i}_{sh}{}^2 = 2K\cdot q\cdot B\left(P_r + P_m\right) \tag{32}$$

B is the detector bandwidth. Another noise source is the thermal noise of the detector or preamplifier combination and the mean square noise current here is

$$\bar{i}_{th}{}^2 = \frac{4k\cdot T\cdot B}{R} \tag{33}$$

k is the Boltzmann constant, T is the absolute temperature and R is the load resistance of photodetector. The shot noise power significantly exceeds thermal noise power under given conditions where the reference power is usually higher. Hence this system is called shot noise limited and produces the best available signal-to-noise ratio. To simplify the model and neglect the thermal noise and quantization noise, the signal-to-noise power ratio can be consequently given by [18,19]

$$SNR = \frac{P_s}{P_n} = \frac{\bar{i}_s{}^2}{\bar{i}_{sh}{}^2} = \frac{2K^2\varepsilon^2 P_r P_m}{2K\cdot q\cdot B\left(P_r+P_m\right)} = \frac{\eta\varepsilon^2 P_r P_m}{h\cdot\nu\cdot B\left(P_r+P_m\right)} \tag{34}$$

K, η, h, ν, B are already-introduced parameters, ε is the efficiency factor. The reference power is usually higher ($P_r >> P_m$), this Eq. (34) simplifies to

$$SNR = \frac{\eta\varepsilon^2 P_m}{h\cdot\nu\cdot B}\left(P_r \gg P_m\right) \tag{35}$$

A factor of $\sqrt{2}$ is particularly attractive as an alternative due to its contribution to noise modulation below and above the carrier frequency. Consequently, a carrier signal with power $P_c \gg P_n$ brings a peak phase deviation caused by the spectral noise power density $P'_n = P_n/B$ in 1 Hz bandwidth according to

$$\Delta\phi' \approx \sqrt{\frac{2P'_n}{P_c}} = \sqrt{\frac{2}{CNR'}} \tag{36}$$

CNR' is the carrier–noise ratio of the photocurrent calculated for B=1 Hz.

The definition of CNR is the ratio of the alternating current component of the detector's output signal to shot noise

$$CNR = \frac{P_{AC}}{\bar{i}_{sh}{}^2} = \frac{4K^2 P_s P_{LO}}{2KqB\left(P_s+P_{LO}\right)} = \frac{2\eta P_s}{h\nu B} \tag{37}$$

Then we get the linkage between the SNR and CNR which is $CNR = 2SNR/\varepsilon^2$. A phase deviation caused by the spectral noise power density in 1 Hz bandwidth is given by $\Delta\phi'_n = \varepsilon/\sqrt{SNR'}$, accordingly SNR' is calculated for B=1 Hz. A phase deviation of the Doppler signal is calculated for the desired calibration points according to

$$\Delta\phi = \frac{4\pi}{\lambda}\Delta s \tag{38}$$

The micro-vibration amplitude of the target which is equal to the amplitude of noise in the spectral distribution is considered as the minimum resolvable displacement. Then we can get

$$\begin{aligned} s_{\text{Gauss}} &= \frac{\varepsilon\lambda\Delta\phi_n}{4\pi} = \frac{N\varepsilon\lambda\sigma_{\text{Gauss}}}{4\pi} \\ s_{\text{Lorentz}} &= \frac{\varepsilon\lambda\Delta\phi_n}{4\pi} = \frac{N\varepsilon\lambda\sigma_{\text{Lorentz}}}{4\pi} \end{aligned} \tag{39}$$

If the value of N is equal to 3, the probability of accurate detection of target vibration is 99.74%.

$$\begin{aligned} s_{\text{Gauss}} &= \frac{3\varepsilon\lambda\sigma_{\text{Gauss}}}{4\pi} = \frac{3\varepsilon\lambda d}{c}\Delta\omega_{Gauss} \\ s_{\text{Lorentz}} &= \frac{3\varepsilon\lambda\sigma_{\text{Lorentz}}}{4\pi} = \frac{3\varepsilon\lambda}{2}\sqrt{\frac{d\Delta\omega_{\text{Lorentz}}}{\pi c}} \end{aligned} \tag{40}$$

Subsequently we can obtain the noise-equivalent mean square displacement

$$\overline{s'}_n = \frac{1}{\sqrt{2}}\cdot\frac{\lambda}{4\pi}\Delta\phi'_n = \frac{1}{\sqrt{2}}\cdot\frac{\lambda\varepsilon}{4\pi\sqrt{SNR'}} \tag{41}$$

It is clear that we have obtained the displacement resolution of different laser oscillation lineshapes for a general heterodyne detection system. It can be concluded that the minimum resolvable displacement is affected by the wavelength of light source, the detection distance and linewidth. However the noise-equivalent mean square displacement is affected by the wavelength of light source and measurement beam power. This can provide a theoretical support for the displacement resolution and engineering application of the heterodyne detection. (See Table 1.)

3. Numerical results

The probability density distribution of phase noise, the power spectrum of photocurrent and the displacement resolution are studied by numerical simulations. The simulation parameters include the wavelength λ of light source, laser linewidth, detection distance and measurement beam power, which are used to obtain the numerical results illustrating our analyses above. According to Eqs. (40) and (41), the displacement resolution is determined by the quantum efficiency η, the efficiency factor ε, the laser wavelength λ, the detection distance and laser linewidth. Firstly, we set some global parameters: $P_r \gg P_m$, the quantum efficiency $\eta = 0.8$, the efficiency factor $\varepsilon = 0.5$, the intermediate frequency $\omega_s = 20$ MHz and the laser wavelength λ=1550 nm. Fig. 3(a–b) shows the power spectrum of photocurrent in the detection distance of 100m. Fig. 4(a–d) illustrates the probability density distribution of phase noise under the different laser lineshapes. Fig. 5(a–d) demonstrates that the minimum resolvable displacement varies with the laser linewidth under different detection distances. And Fig. 6 suggests that the noise-equivalent mean square displacement for

Table 1
Minimum resolvable displacement for different oscillation lineshape.

	Oscillation lineshape	Variance of phase noise	Minimum resolvable displacement
1	Lorentz	$\sigma^2_{\text{Lorentz}} = 2\pi\Delta\omega_{\text{Lorentz}}\tau_d$	$s_{\text{Lorentz}} = \frac{3\varepsilon\lambda}{2}\sqrt{\frac{d\Delta\omega_{\text{Lorentz}}}{\pi c}}$
2	Gauss	$\sigma^2_{\text{Gauss}} = (2\pi\Delta\omega_{\text{Gauss}})^2\tau_d^2$	$s_{\text{Gauss}} = \frac{3\varepsilon\lambda d}{c}\Delta\omega_{\text{Gauss}}$

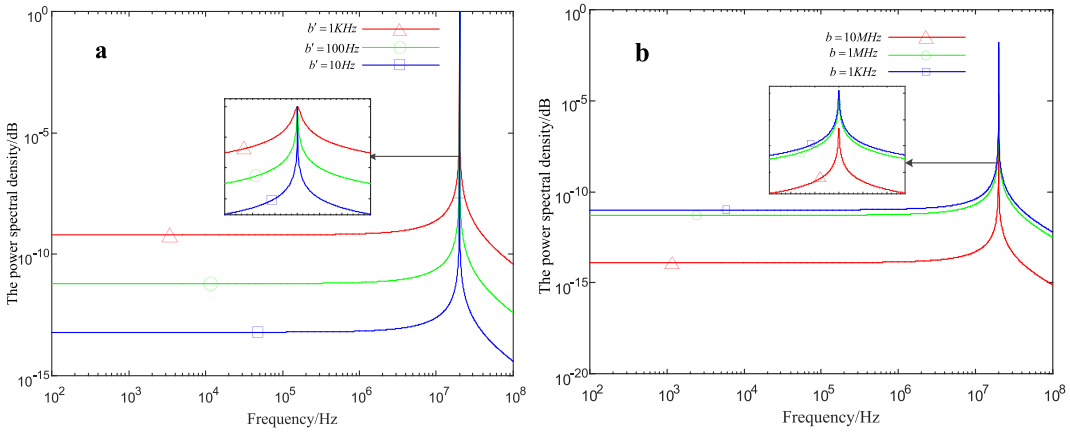

Fig. 3. The power spectral distribution for a photocurrent varies with laser linewidth (a) or linewidth fluctuations (b)

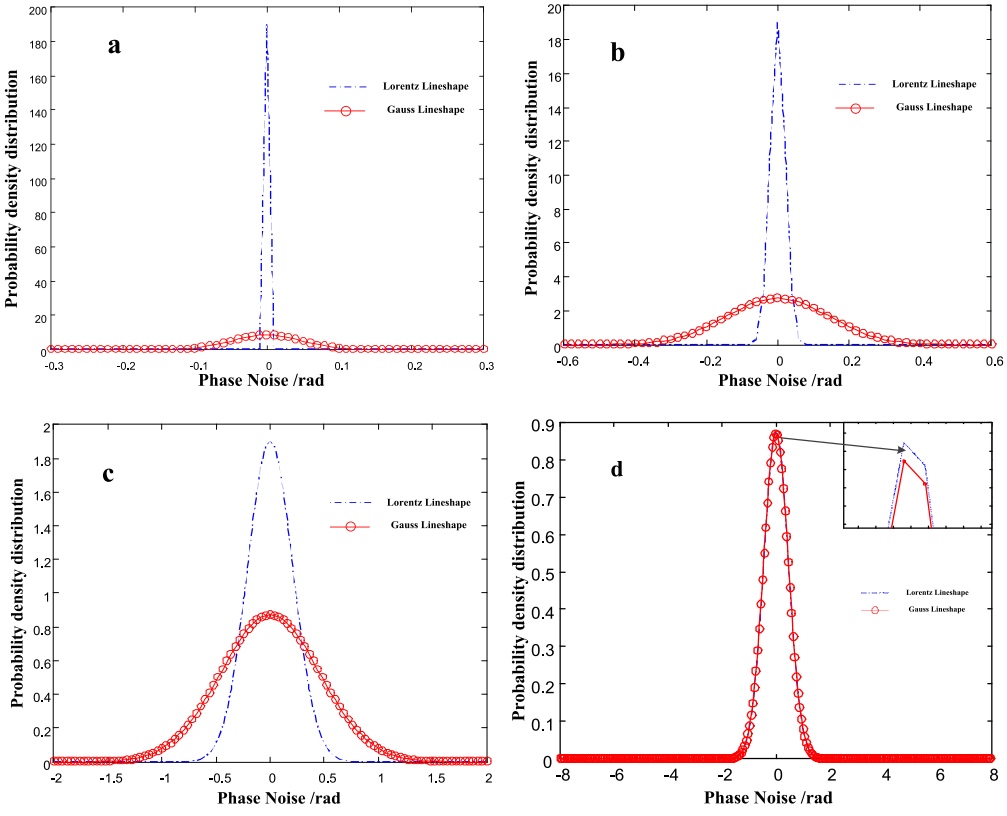

Fig. 4. The probability density distribution of phase noise in the detection distance of 100 m.

B=1 Hz varies with the measurement beam power according to the spectral signal-to-noise power ratio Eq. (35).

Fig. 3 illustrates the power spectral distribution of photocurrent for a linewidth of 1 kHz and a detection distance of 100 m. The relative ratio of power in Fig. 3(a) has variations (in comparison with the maximum power) with frequency fluctuations. The linewidth fluctuation b' is smaller, the spectral lineshape is closer to the Lorentz lineshape. And the linewidth fluctuation has no effects on the spectral peak value. For that, in Fig. 3(b) we get simulation results of the power spectral variations with laser linewidth. We found that when the laser linewidth $b \ll 1$ MHz, its impact on the power spectrum is very slight. But if b approaches or exceeds MHz, it has a significant impact on the power spectrum. Besides, the value of b do not change the lineshape of the power spectrum. The two terms lead to quite different power spectrums from the Eq. (23).

Fig. 4 shows that the probability distribution model of phase noise obeys a Gaussian distribution. The linewidths of Gauss lineshape and Lorentz lineshape in Fig. 4(a–c) keep consistent, which are 1 kHz, 10 kHz and 100 kHz respectively. In Fig. 4(d) the linewidth of Gauss lineshape

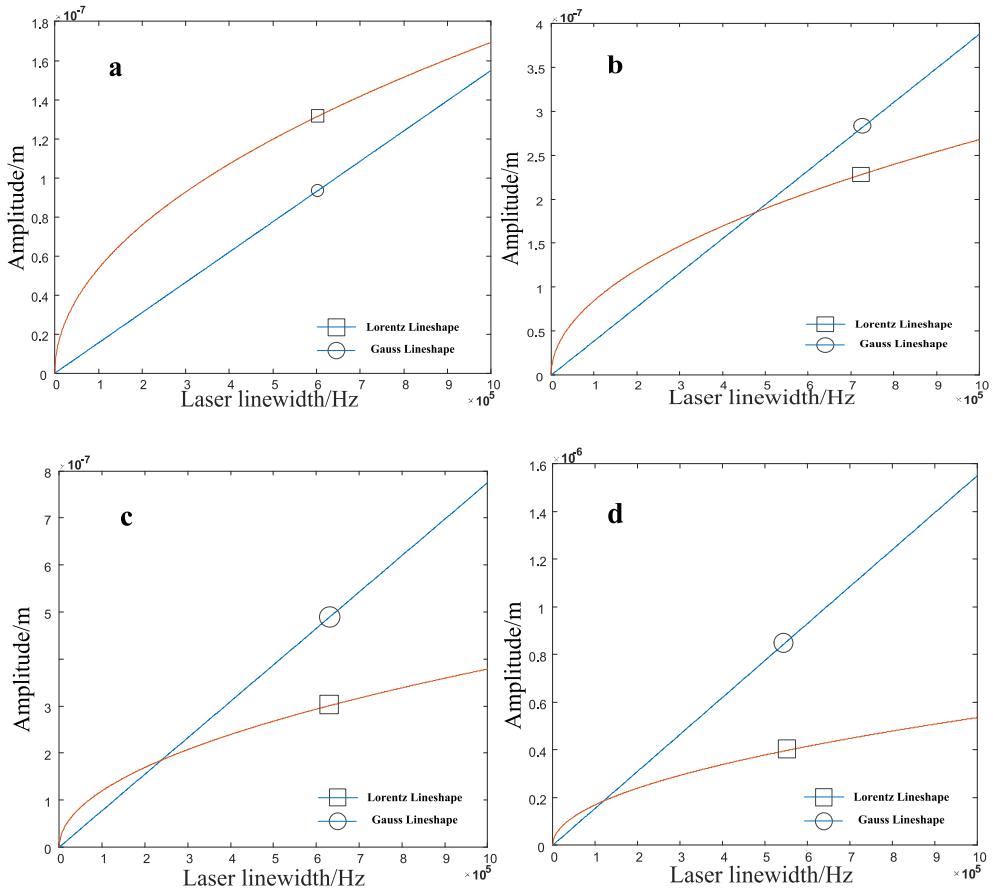

Fig. 5. Minimum resolvable displacement varies with the laser linewidth under the different detection distance. Detection distance of (a–d) is 20 m, 50 m, 100 m, 200 m, respectively.

is 218 kHz and the linewidth of Lorentz lineshape is 100 kHz. Obviously, there is a certain linewidth value making two different lineshapes coincided and then two laser sources bring the same phase noise—this means that laser source has same impacts on the displacement resolution. Besides, for the linewidth of 1 kHz, 5 kHz, 80 kHz and 1 MHz of Lorentz lineshape, the ratio of $\Delta\omega_{\text{Gauss}}/\Delta\omega_{\text{Lorentz}}$ making two lineshapes coincided are about 21.8, 9.78, 2.44, and 0.69, respectively. Generally speaking, there are significant differences among laser sources with the same linewidth but different lineshape. We can use numerical results to select appropriate laser source so as to achieve the higher displacement resolution.

Fig. 5 demonstrates that the minimum resolvable displacement increases as the laser linewidth increases. The abscissa of crossing point decreases as the detection distance increases, which indicates the laser linewidth with the same minimum resolvable displacement. The smaller the abscissa of crossing point, the larger the detection distance. However, if we want to achieve a long-range heterodyne detection we have to take into account the atmospheric turbulence. Therefore it is evident that we should select the appropriate laser source overall considering laser linewidth, detection distance and the wavelength of light source for different precision requirements.

Fig. 6 suggests that the noise-equivalent mean square displacement is inversely proportional to the root-mean-square of measurement light power. When measurement beam power $P_m = 0.1$ mW, 0.01 mW, 1μ W, the noise-equivalent mean square displacement is 3.5×10^{-15} m/$\sqrt{\text{Hz}}$ 1.1×10^{-14} m/$\sqrt{\text{Hz}}$, 3.5×10^{-14} m/$\sqrt{\text{Hz}}$, respectively.

Based on above theoretical analyses and numerical results, the limited displacement resolution of the heterodyne detection is studied in detail. If we want to achieve the higher displacement resolution, we have to narrow the linewidth, reduce the detection distance or shorten the laser wavelength. Besides, the displacement resolution has heavy

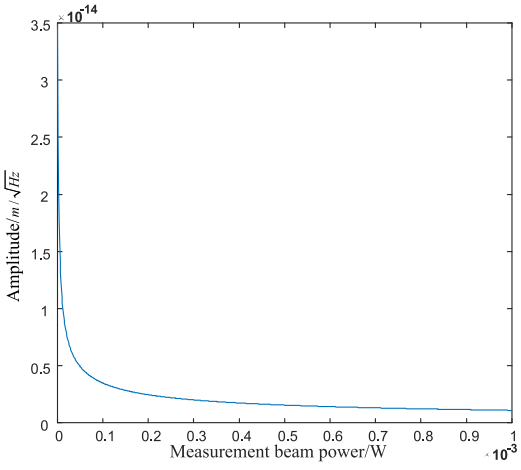

Fig. 6. The noise-equivalent mean square displacement varies with measurement beam power.

dependence on laser oscillation lineshapes. The results of theoretical analyses and numerical simulations match each other.

It should be noted here that the preceding calculations of noise limited resolution are estimations of the physical limits. In reality, there are additional broadband noise and spurious noise components in the heterodyne detection, which may push the practical limits of displacement resolution to a lower level. As mentioned, the high resolution is feasible only under the provision of sufficiently small resolution bandwidth of the subsequent signal acquisition system or

using an adequate number of averages. This is usually not a problem when analyzing stationary vibrations or repetitive dynamic processes.

4. Conclusion

Based on the Wiener–Khinchin theorem, the power spectral density has been derived to evaluate the performance of the optical heterodyne detection system. According to the probability distribution of the phase noise, we build up the physical models of the minimum resolvable displacement and the noise-equivalent mean square displacement with the key parameters including the laser wavelength, the detection distance, the laser linewidth and signal power. We conclude that the noise-equivalent mean square displacement is inversely proportional to the root-mean-square of measurement light power. The noise-equivalent mean square displacement can reach 3.5×10^{-15} m/$\sqrt{\text{Hz}}$ under the given parameters. This can provide a theoretical reference for the displacement resolution and engineering application for micro-vibration measurement by the heterodyne detection technique.

Acknowledgments

This work was supported by the following research grants: Key Research Program of Frontier Science, CAS (Grant No. QYZDB-SSW-SLH014) and the Yong Scientists Fund of the National Nature Science Foundation of China (Grant No. 61205143).

Appendix A. Random variables

If we are dealing with a Gaussian random variable then we must remember that the rules of addition and subtraction are different from normal. Consider a random variable $N_X\left(\mu,\sigma^2\right)$ where $N_X\left(\mu,\sigma^2\right)$indicates a random variable with a normal distribution with the expected value μ and the varianceσ^2.

$$f\left(x\right)=\frac{1}{\sqrt{2\pi\sigma^2}}e^{-(x-\mu)^2/(2\sigma^2)}$$

If we transform the variable $X \rightarrow aX + c$ we can equivalently write this as $N_X\left(a\mu+c, a^2\sigma^2\right)$. Now consider two statistically independent variables X and Y

$$X \pm Y = Z$$

$$\equiv N_X\left(\mu_X,{\sigma_X}^2\right) \pm N_Y\left(\mu_Y,{\sigma_Y}^2\right) = N_Z\left(\mu_X \pm \mu_Y, {\sigma_X}^2+{\sigma_Y}^2\right)$$

$$XY = Z$$

$$\equiv N_X\left(\mu_X,{\sigma_X}^2\right) N_Y\left(\mu_Y,{\sigma_Y}^2\right) = N_Z\left(\mu_X\mu_Y, \mu_X^2{\sigma_X}^2+\mu_Y^2{\sigma_Y}^2\right)$$

$$X/Y = Z$$

$$\equiv N_X\left(\mu_X,{\sigma_X}^2\right)/N_Y\left(\mu_Y,{\sigma_Y}^2\right) = N_Z\left(\mu_X/\mu_Y, \frac{\sigma_X^2}{Y^2}+\frac{X^2}{Y^4}{\sigma_Y}^2\right)$$

The last case is not strictly true since a division of two Gaussian variables leads to a Cauchy distributed random variable. In general for a function of statistically independent Gaussian white noise variables, we have

$$f\left(X,Y,Z\right)$$

$$\sigma_f^2 \approx \left(\frac{\delta f}{\delta X}\right)^2\delta_X^2+\left(\frac{\delta f}{\delta Y}\right)^2\delta_Y^2+\left(\frac{\delta f}{\delta Z}\right)^2\delta_Z^2$$

However, if the variables are correlated, then we should use for example

$$aX \pm bY = Z$$
$$\sigma_Z^2 = a^2\sigma_X^2+b^2{\sigma_Y}^2 \pm 2ab\text{cov}_{AB}$$

$\text{cov}_{AB} = E\left[\left(A-\overline{A}\right)\left(B-\overline{B}\right)\right]$. We can now consider the case

$$X + X = Z$$

and find that

$$\sigma_Z^2 = \sigma_X^2+\sigma_X^2+2\sigma_X^2 = 4\sigma_X^2,$$

which is what we would expect for

$$2X = Z$$

In the derivations of this note, we most often add or subtract two statistically independent variables with means of zero and the same variance

$$N_X\left(0,\sigma_\tau^2\right)+N_Y\left(0,\sigma_\tau^2\right)=N_Z\left(0,2\sigma_\tau^2\right),$$

which leads to the slightly contra-intuitive statement

$$N_X\left(0,\sigma_\tau^2\right)+N_Y\left(0,\sigma_\tau^2\right)=\sqrt{2}N_Z\left(0,\sigma_\tau^2\right)$$

This topic is known as the ‘propagation of uncertainty’ and can be found in many books. In the most general case, we would need to construct a matrix of the correlations between the variables in order to calculate the error accurately.

References

[1] H.A. Deferrari, F.A. Andrews, Laser interferometric technique for measuring small-order vibration displacements, Acoust. Soc. Am. J. 39 (1966) 979–980.
[2] H.A. Deferrari, R.A. Darby, F.A. Andrews, Vibrational displacement and mode-shape measurement by a laser interferometer, J. Acoust. Soc. Am. 42 (1967) 982–990.
[3] F.J. Eberhardt, F.A. Andrews, An optical heterodyne system for measurement and analysis of vibration, J. Acoust. Soc. Am. 47 (1970) 116.
[4] A.C. Lewin, A.D. Kersey, D.A. Jackson, Non-contact surface vibration analysis using a monomode fibre optic interferometer incorporating an open air path, J. Phys. E Sci. Instrum. 18 (2000) 604.
[5] N.A. Halliwell, C.J.D. Pickering, P.G. Eastwood, The laser torsional vibrometer: A new instrument, J. Sound Vib. 93 (1984) 588–592.
[6] E.A. Swanson, G.M. Carter, D.J. Bernays, D.M. Hodsdon, Optical spatial tracking using coherent detection in the pupil plane, Appl. Opt. 28 (1989) 3918.
[7] C.L. Matson, Applications of the HI-CLASS (high-performance CO2 laser radar surveillance sensor) laser system for active imaging of space objects, Proc. SPIE - Int. Soc. Opt. Eng. 3380 (1998) 243–249.
[8] A.M. Bauer, F. Ritter, G. Siegmund, High-precision laser vibrometers based on digital Doppler signal processing, Proc. SPIE 4827 (2002) 50–61.
[9] F. Fang, Y. Zhang, D. Zhou, G. Zhang, Principle of AOM laser heterodyne measuring and its instrument, Proc. SPIE - Int. Soc. Opt. Eng. 2899 (1996) 599–602.
[10] C. Li, T. Wang, H. Zhang, J. Xie, L. Liu, Z. Shuai, G. Jin, The performance of heterodyne detection system for partially coherent beams in turbulent atmosphere, Opt. Commun. 356 (2015) 620–627.
[11] M. Salem, J.P. Rolland, Heterodyne efficiency of a detection system for partially coherent beams, J. Opt. Soc. Am. A 27 (2010) 1111–1119.
[12] A. Dang, H. Guo, L. Liu, Y. Ren, Heterodyne efficiency of a coherent free-space optical communication model through atmospheric turbulence, Appl. Opt. 51 (2012) 7246.
[13] A. Siegman, B. Daino, K. Manes, Preliminary measurements of laser short-term frequency fluctuations, IEEE J. Quantum Electron. 3 (1967) 180–189.
[14] H.K. Teng, K.C. Lang, Heterodyne interferometer for displacement measurement with amplitude quadrature and noise suppression, Opt. Commun. 280 (2007) 16–22.
[15] P.B. Gallion, G. Debarge, Quantum phase noise and field correlation in single frequency semiconductor laser systems, IEEE J. Quantum Electron. 20 (1984) 343–349.
[16] D. Uttam, B. Culshaw, Precision time domain reflectometry in optical fiber systems using a frequency modulated continuous wave ranging technique, J. Lightwave Technol. 3 (1985) 971–977.
[17] Y. Painchaud, M. Poulin, M. Morin, M. Têtu, Performance of balanced detection in a coherent receiver, Opt. Express 17 (2009) 3659–3672.
[18] C. Rembe, G. Siegmund, H. Steger, M. Wörtge, Optical inspection of microsystems, 2007.
[19] J.R. Ohm, H.D. Lüke, Analoge Modulationsverfahren, Springer, Berlin, Heidelberg, 2014.